

BUCKLING AND POST-BUCKLING PERFORMANCE OF STIFFENED WEBS SUBJECTED TO INTERACTIVE SHEAR AND COMPRESSION

N Hussain* and J Loughlan**

*School of Mechanical Engineering and Design, London South Bank University, UK
Corresponding Author: E-mail: N.Hussain@Lsbu.ac.uk

**Department of Aeronautical and Automotive Engineering, Loughborough University, UK
E-mail: J.Loughlan@Lboro.ac.uk

Keywords: Stiffened plates; Combined loading; In-plane shear and compression; Post-buckling; Elasto-plastic unloading; Two-dimensional design curves.

Abstract. This paper examines the buckling and post-buckling response of stiffened plates with centrally located single and two equidistant stiffeners under combined shear and compression. The introduction of stiffening elements considerably improves the buckling and post-buckling performance of thin plates when subjected to interactive loading. This is mainly due to the flexural and torsional rigidities of the stiffening elements that lead to a more stabilised structural system. This work essentially outlines the finite element modelling procedures that are employed to determine the critical buckling and nonlinear post-buckling response of stiffened web panels under combined shear and compression respectively. The modelling strategies and solution procedures, detailed in this paper, have shown to be able to describe the complete loading history of the actively applied load, in the presence of a constant shear preload, from the onset of initial buckling through the elastic and elasto-plastic post-buckling phase of behaviour to the ultimate conditions followed by the subsequent elasto-plastic unloading phase. The validity of this approach is ascertained by obtaining a good comparison against the exiting FEM results present in the literature.

1 INTRODUCTION

Stiffened plating is used widely in many disciplines of engineering with applications to be found in mechanical, civil, aeronautical, and marine engineering to name some. Stiffened panels are efficient structural elements which readily contribute to the light-weighting of large structural systems and which can be tailor designed with the appropriate strength and stiffness requirements for any particular application. In practice, stiffened panels are more than likely to be subjected to complex, combined in-plane and lateral loading systems such as that which would be experienced in the wing structure of a large civilian airliner or in the hull structure of a large ship. Our knowledge and understanding of the structural performance and failure mechanics of stiffened plating under complex loading is at a fairly sophisticated level at present due to the wide body of research that has been carried out over the years. Today's research continues to advance our knowledge and to contribute significantly to the efficient design of stiffened plate structural systems. The considerable advances made in finite element software and computing technology have been influential in aiding progress. These have evolved to such a sophisticated level that today we are verging on the possibility of virtual testing to aid us in our quest for safe, reliable and efficient structural designs.

Many researchers have investigated the effect of utilising transverse and longitudinal stiffeners on buckling and post-buckling response and on the failure mechanics of thin-walled stiffened plate structural systems. Plank and Williams [1] have studied the behaviour of stiffened panels with different stiffener geometries. The panels were subjected to combined

shear and compressive loading and useful interaction curves were obtained which reflected the influence of the different stiffener geometries.

Bulson [2] applied analytical techniques to determine the critical buckling response of square and long plates with simply supported and clamped boundary conditions under various loading patterns such as shear, compression, bending and their combinations.

Loughlan [3] presented a finite strip formulation to determine the critical buckling stress and natural frequencies of vibration for metallic shear loaded stiffened panels. This work illustrated the significant influence of in-plane shear loading on the natural frequencies of vibration of the panels and was able to demonstrate the well-known fact that when the applied shear is critical, the natural frequency of the panel becomes zero.

Loughlan [4] studied the behaviour of carbon fibre composite stiffened panels subjected to combined in-plane compression and shear loading using the finite strip method. Interaction curves were obtained from this work and the influence of the bending and torsional stiffnesses of the stiffeners on the critical buckling levels was outlined in detail.

Ueda et al. [5] investigated the behaviour of stiffened flat rectangular plates with the stiffeners employed in the longitudinal direction. The stiffened plates were subjected to combined biaxial compression and shear loading and appropriate interaction expressions were developed to describe the buckling and ultimate capacity of the plates under the combined loading.

Lee et al. [6] have investigated the behaviour of transverse stiffeners attached to shear web panels through a three-dimensional nonlinear finite element analysis. It was found from this work that the intermediate transverse stiffeners attached on shear web panels are not necessarily subjected to axial compression in the postbuckling range of behaviour, and as a result, it was suggested by these researchers that the requirement for minimum stiffener areas in current design specifications could be relaxed or eliminated.

Lee et al. [7] conducted an experiment in order to investigate the behaviour of the intermediate transverse stiffeners during postbuckling. The test results confirmed their earlier findings [6] and a new design rule for the sizing of the transverse stiffeners was formulated through extensive nonlinear finite element analysis data verified by test results.

Xie and Chapman [8] developed a design formula for predicting the axial forces in actual stiffeners with a finite axial rigidity. This was achieved by incorporating coefficients which were determined by means of non-linear finite element results produced using the general-purpose FE program abaqus. The non-deflecting stiffener model with finite axial rigidity is shown in this work to provide a sufficiently accurate estimation of the axial force in a real stiffener.

A computational model for the analysis of the global buckling and post-buckling of stiffened panels has been derived by Byklum et al. [9]. The model is formulated using large deflection plate theory and energy principles. The procedure is semi-analytical in nature and any combination of biaxial in-plane compression or tension, shear, and lateral pressure may be analysed. The load-deflection curves produced by the proposed model are compared with results from nonlinear finite element and good correspondence is illustrated.

Alinia [10] used the finite element method to study the buckling performance of stiffened plates subjected to in-plane shear loading with a particular emphasis on the optimal aspects of the stiffener design. This work concluded that to achieve optimum panel designs, the optimal flexural stiffness ratio of the stiffener to the plate corresponds to the point where the buckling mode changes from overall buckling to local buckling. It was also suggested that the number of panels produced due to the utilisation of intermediate stiffeners should not be less than the overall aspect ratio of the plate.

Murphy et al. [11] have demonstrated that using a commercial implicit code, the finite element method can be used successfully to model the post-buckling behaviour of flat aircraft riveted panels subjected to shear loading. This work develops appropriate modelling procedures for the flat riveted panels investigating element selection, mesh density idealisation and material modelling selection, with the obtained results being validated against mechanical tests. The work has also generated a series of guidelines for the non-linear computational analysis of flat riveted panels subjected to uniform shear loading.

Featherston et al. [12] carried out an experiment to examine the buckling and postbuckling behaviour of a stiffened panel loaded in-plane to produce a combination of shear, compressive and in-plane bending stresses. Of particular interest was the transfer of load from the plates, constituting this panel, into the stiffeners at higher loads. The stiffened panel structure was seen to behave in a stable manner in the postbuckling period and was shown to be capable of supporting loads in excess of four times the initial buckling load. A relatively simple nonlinear finite element analysis was shown to accurately predict this behaviour at up to twice the initial buckling load.

Paik [13,14] carried out finite element studies to determine the ultimate load capacity of simply supported plates subjected to shear and combined shear and biaxial compression and for the case of the straight edge boundary condition. The effect of hole size, plate aspect ratio, and plate slenderness ratio on ultimate conditions was detailed in this work and a useful design formula was proposed for determining the ultimate capacity of perforated plates as a function of the hole size and the plate dimensions.

Alinia and Shirazi [15] proposed design formulations by presenting a parametric study to evaluate the optimal dimensions of single sided flat stiffeners utilised in steel plate shear walls. By carrying out finite element analysis it was observed that there exists a certain relation between optimal thickness, height of the stiffener and plate dimensions. It was also illustrated with the help of nonlinear analysis that the post buckled reserved remained almost the same for various optimal dimensions of stiffeners.

Loughlan and Hussain [16] presented the finite element modelling strategy used to predict the post-buckling behaviour of the stiffened panels under shear displacement loading. They showed the transition buckling stage between general to local buckling as the rigidity of the stiffener approaches the critical level. The transitional buckled mode is predominantly associated with the shear web plate and the stiffener line is close to, but not quite, a nodal line.

The work presented in this paper is that of numerical simulation with the view to developing accurate and reliable modelling strategies and solution procedures, which will predict the critical buckling and postbuckling response of stiffened webs under combined shear and compression. Two-dimensional design interaction curves, based on buckling performance, are shown with limiting boundaries shown to be the critical combinations of the applied loading for different structural configurations. In the case of incremental nonlinear analysis, two-dimensional design curves with limiting boundaries are based on the ultimate combinations of the applied loading for different structural configurations. This paper details the suitable finite element modelling strategies and procedures that are capable of accurately predicting the buckling as well as post-buckling structural response of the stiffened webs with centrally located single and two equidistant stiffeners under combined shear and compression.

2. FINITE ELEMENT MODELLING

The finite element simulation package PATRAN/NASTRAN is used to determine the elastic critical buckling and post-buckling elasto-plastic response of the stiffened webs under interactive loading. The simulations use the four-noded CQUAD4 quadrilateral shell element

of the package to discretise the thin webs in order to build the finite element models for the eigenvalue and incremental nonlinear analyses. The CQUAD4 shell element is particularly well suited for dealing with the post-buckling behaviour of thin-walled structural systems. It is readily able to account for the interaction of the local bending and membrane stretching of the webs, which takes place during the post-buckling process. The size of the elements is an important factor in the simulation process, a fine mesh provides greater flexibility and leads, generally, to more accurate solutions however, the greater the number of elements, the more computational time is required and so appropriate convergence studies are necessary to obtain the most optimised accurate solution. The modelling details for the elastic buckling problem in MSC NASTRAN are different to that of nonlinear post-buckling problem as shown in the following sections.

2.1 Finite Element Modelling – Elastic Buckling

2.1.1. Geometry and Material Properties

The skin dimensions of the rectangular stiffened panel are 1000 mm by 500 mm with a uniform thickness of 2mm. The geometry of the stiffener considered is that of the plain flat outstand. The thickness of the stiffener is 2mm and its depth is varied to study the influence of the stiffener on the critical buckling and post-buckling performance. Plain flat outstands on one side of the web plate have been considered. The element size used in the stiffened panel simulations is 16.67 mm for the plate as well as for the stiffener. The simplified von-Mises elastic-perfectly plastic material model is used for the isotropic aluminium material with an elastic modulus of $71.7 * 10^3$ N/mm², Poisson ratio of 0.33 and yield stress values of 300, 400 and 500 N/mm².

2.1.2. Boundary and Loading Conditions

Simply supported boundary conditions are used in which the translations of the four edges of a web panel are constrained in Z-direction i.e. normal to the plane of the plate as shown in figure 1. Moreover the movement of bottom left and right corner nodes is fixed in X & Y-direction and in Y-direction respectively. In other words the bottom left node is completely fixed i.e. in X, Y and Z-directions whereas the bottom right node is considered to be on a roller and can only translate in X-direction.

It is noted that the bending moment due to the application of shear load to the skin only does not produce notable out-of-plane deflections prior to initial buckling. Therefore, eccentric shear load is applied only to the skin of the stiffened web panel in the form of uniformly distributed load (UDL). The transverse compression in the form of UDL is applied to the top and bottom edges of the skin as well as to stiffener as illustrated in figure 1 in order to avoid the bending moment action.

The accurate application of combined loading is achieved by executing the STATSUB command of MSC NASTRAN. Two load cases are created for instance ‘Shear’ and ‘Compression’ in the module of ‘Load case’ present in MSC PATRAN. In both ‘Shear’ and ‘Compression’ load cases the displacement boundary conditions are included as well as uniformly distributed shear and compression load respectively. One load is considered as constant preload whilst other as active load regardless of shear or compression. The choice of constant preload and active load does not affect the final results. In the present analysis, the shear load is selected to act as a constant preload while compression is applied as an active load. The subcases of similar names as of the load cases are automatically generated and can be viewed in the forms of ‘Subcases’ and ‘Subcase Select’ present in the ‘Analysis’ module of MSC PATRAN. In order to make shear as a constant preload, a linear static solution is run while pure shear load is applied to the stiffened web panel prior to the buckling analysis. The

linear static solution sequence (SOL 101) is selected from the ‘Solution Type’ form and a ‘Shear’ subcase from the ‘Subcase Select’ form. When the linear static solution is completed the solution sequence is changed from linear static (SOL 101) to buckling (SOL 105) in the ‘Solution Type’ form present in the ‘Analysis’ module of MSC PATRAN. It is of note that an additional subcase is generated and can be observed in the ‘Subcase Select’ form with a prefix of (preload) such as in the present case ‘(preload)Shear’. To obtain a buckling solution under combined loading two subcases are selected in ‘Subcase Select’ form first ‘(preload)Shear’ and second ‘Compression’. After the completion of buckling solution the first eigenvalue obtained is multiplied only to the applied transverse compression in order to get a value of critical compressive buckling stress in the presence of a constant applied shear preload. Once the ‘(preload)Shear’ subcase is created the value of constant shear preload is only to be changed to different levels to obtain the corresponding critical compressive buckling stress.

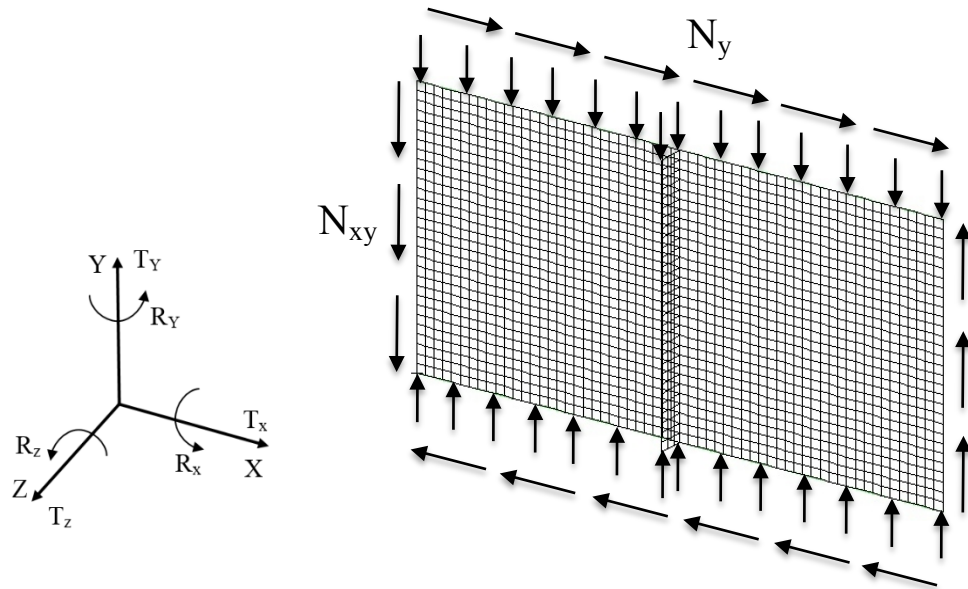


Figure 1: Discretised web panel with single asymmetrical stiffener under combined compression and shear loading.

2.2. Finite Element Modelling – Nonlinear Post-buckling

2.2.1. Geometry and Material Properties

Geometry, element type and element size used in the post-buckling analysis of stiffened web panels remained same as described in section 2.1.1. However, the uniform thickness of the skin and the stiffener is of 6.25 mm. The depth of stiffener is varied to investigate its influence on the post-buckled response of asymmetrically stiffened web panels.

The simplified von-Mises elastic-perfectly plastic material model is used for the isotropic steel material with an elastic modulus of $207.338 * 10^3$ N/mm², Poisson ratio of 0.3 and yield stress value of 352.8 N/mm².

2.2.2. Boundary and Loading Conditions

Simply supported boundary conditions are utilised in which the translations of the four edges of a web panel are constrained in the Z-direction i.e. normal to the plane of the plate. The movement of the bottom edge of the web panel is completely fixed in both X and Y-directions. The boundaries of the web panel are kept straight in-plane throughout the analysis

by employing the multipoint constraints in the form of RBE2 elements. The motion of the bottom edge of the web is already completely fixed i.e. X, Y and Z-directions and thus the RBE2 elements are utilised on remaining three edges in order to enforce the boundaries to remain straight in the plane of the plate. The middle node of each web boundary (except the bottom edge) of the web plate is chosen to act as master node as shown in figure 2. The master node of the top edge is denoted by MN-1 and similarly the master nodes of left and right boundaries are denoted by MN-2 and MN-3 respectively. The remaining nodes present at these three edges are considered to be the slave nodes and are connected to their respective master node at each edge. Two degrees of freedom, which are translation in Y-direction (T_y) and rotation about the axis normal to the web surface (R_z), are associated with the set of slave nodes of the top edge including the nodes present at top right and left corners of the web plate. The degrees of freedom attached to the sets of slave nodes of right and left edges of the web (excluding web corner nodes) are translation in X-direction (T_x) and rotation about Z-axis (R_z). In this way, the web boundaries are kept remain straight in the plane of the plate; however, they are free to translate in-plane as well as to rotate about the Z-axis.

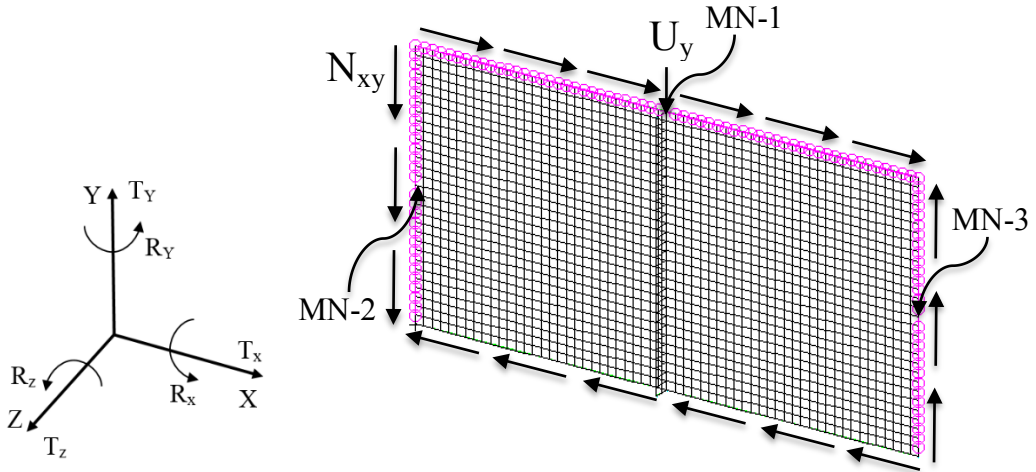


Figure 2: Discretised web panel with single asymmetrical stiffener under combined compression and shear loading.

Shear loading (N_{xy}) is applied at the web boundaries in the form uniformly distributed load (UDL). Whereas compression (U_y) is applied at the top edge of the web in the form of enforced displacement and it is clear from figure 2 that the compressive displacement is shown to be applied only at the master node (MN-1). Moreover, figure 2 illustrates that the combined shear and compression loadings are applied only to the skin of the stiffened web panel. In order to evaluate the compressive stress, once the solution is completed, the component of multipoint reactive force in the Y-direction is extracted from the data for the master node (MN-1) and is further divided by the cross sectional area of the longer edge of the panel where the compression is applied. This compressive stress is referred as average transverse compression (σ_{yav}). In the current post-buckling analysis the shear is chosen to be a constant preload acting right from the beginning of the nonlinear solution procedure and the value of applied shear load in each run remains unchanged throughout the solution, whilst, compression is considered to be an active loading and is incremented throughout the solution run.

The load cases, which are set up for the application of combined loading, group together the boundary and interactive loading conditions and are utilised in a specific way to keep the

shear preload constant as well as to increment compression alone throughout the nonlinear analysis. In ‘Load Cases’ module of MSC PATRAN there is an option of a ‘Load Case Scale Factor’ and the value of this factor is in fact multiplied to the entire group of boundary and loading conditions present within the load case. The default value of ‘Load Case Scale Factor’ is 1.0, which is kept unchanged for the load cases used in the current analysis. Any displacement or loading condition present within the load case can also be multiplied individually by inserting a scale factor in the ‘Input Data’ form. Up to this point the applied loading has been partitioned by changing the default value of the ‘Load Case Scale Factor’ to different numerical numbers in order to carry out the complete incremental nonlinear static analysis. However, in the current strategy the value of shear loading, which is acting as a constant preload, needs to remain unchanged throughout the solution whilst the transverse compression is being continually incremented. Therefore instead of multiplying the entire load case with a ‘Load Case Scale Factor’, which would ultimately increment everything within the load case including the shear loading, the transversely applied compressive displacement is individually multiplied by a scale factor. The value of scale factor associated with all other boundary and loading conditions excluding the transverse compression within the load case remains unchanged.

The number of increments specified in the NINC field of every subcase is changed to 1. The primary difference in the aforementioned strategy is that every subcase is considered itself as an increment unlike the previous approaches where the number of equally sized increments within each subcase was defined by inserting a nonzero value in the NINC field. The scale factor that is associated with the transverse compression within the load case can be varied in order to change the size of increments from one subcase to other. Full Newton-Raphson incremental iterative scheme is employed to accurately predict the complex structural response under the combined shear and compression loading by taking accurately into account the high degree of geometric and elasto-plastic material nonlinearities. The facilities of SOL105 & SOL 106 of MSC NASTRAN are exploited to perform the elastic buckling and elasto-plastic post-buckling analysis.

However, there are situations where the numerical solution seems to terminate due to the unexpected structural response for instance sudden change of buckle mode shape. In order to overcome these peculiarities the number of increments linked with the subcase/subcases in the region where problem exists can be increased from 1 to higher number. By doing so, the compression, which is already a small increment, is further incremented along with the shear loading within the subcase but shear loading as described earlier needs to remain at a constant level throughout the nonlinear solution. The increased number of increments does not appear in the output results after the completion of nonlinear analysis if the intermediate output option in the ‘Advanced’ form type of ‘output requests’ associated with the nonlinear static solution sequence (SOL106) in the ‘Analysis’ module of PATRAN is switched to ‘No’ for the corresponding subcase/subcases. Therefore despite the increased number of increments within the subcase/subcases the final result outcome is found to correspond to both the applied transverse compression (specified by the scale factor within the load case) and the constant level of shear preload.

An extremely small magnitude of initial geometric imperfection is mapped on the structure to initiate the out-of-plane deflection in the elasto-plastic post-buckling range. The mapped mode shape is obtained from the critical buckling solution of the stiffened panel under pure compression. Therefore, the stiffened web plates are actually considered to be geometrically perfect structures.

3. BUCKLING RESPONSE OF STIFFENED PANELS

3.1. Discussion of Results

The finite element strategy is applied to the web plates to compare the elastic buckling results with the analytical work of Bulson [2] in order to validate the proposed modelling approach. Figure 3 illustrates the comparison and it is of note that the results from finite element modelling denoted by full lines are very close to the Bulson's analytical results represented by dotted lines. These results are for simply supported square and rectangular plates subjected to the combined shear and transverse compression. τ_{xy}/τ_{cr} is seen to be plotted against the σ_y/σ_{cr} where τ_{xy} and σ_y are uniformly applied shear and transverse compressive stresses respectively. Both τ_{cr} and σ_{cr} denote the critical shear buckling stress (in the absence of compression) and critical compressive buckling stress (in the absence of applied shear) respectively. Φ is termed as aspect ratio of the plate and it is defined as the ratio of longer side to the shorter side of a web plate (a/b).

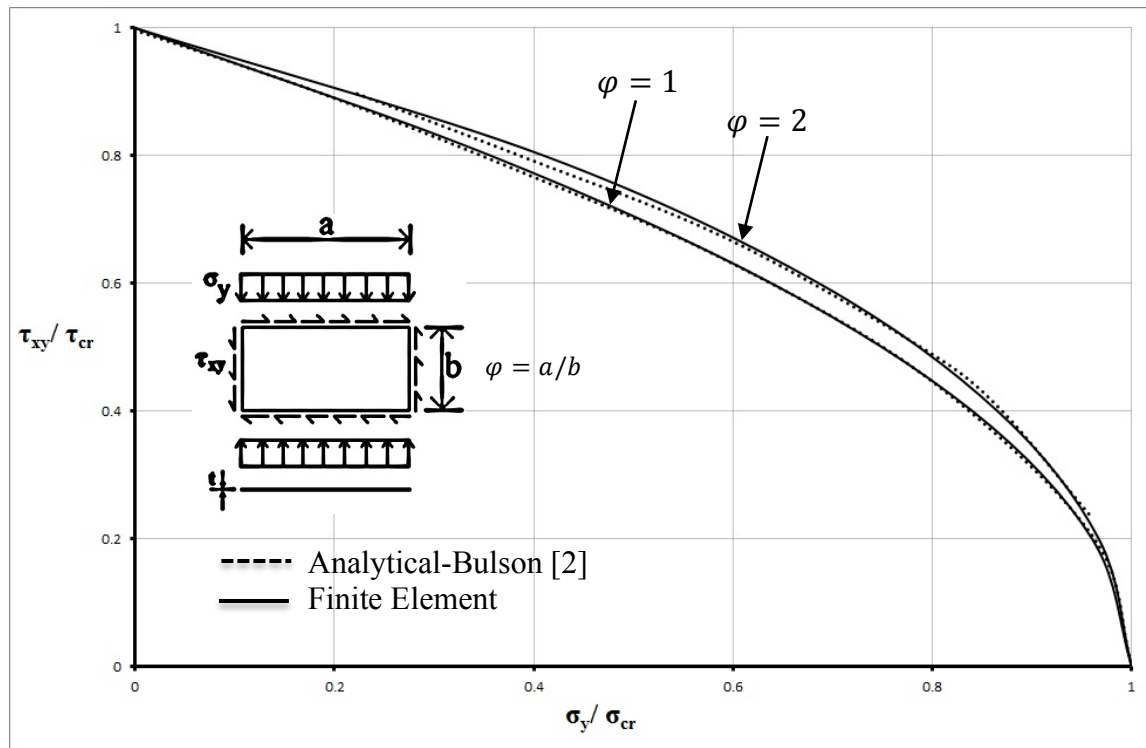


Figure 3: Comparison of FE results with the analytical results of Bulson [2] for simply supported web plates under combined shear and compression.

Figure 4 highlights the independent compressive and shear buckling performance of the stiffener web panels with centrally located single asymmetrical stiffener prior to the application of combined shear and compression. The ratio of critical compressive buckling stress for stiffened panel to that of un-stiffened web plate, $\frac{\sigma_{ycr}}{\sigma_{ycr-unstiffened}}$, and similarly the ratio of critical buckling shear stress of stiffened panel to that of un-stiffened panel, $\frac{\tau_{xycr}}{\tau_{xycr-unstiffened}}$, is seen to be plotted against the stiffener to web depth ratio, d/b . The sole purpose of plotting the non-dimensional stress ratios is that the shear and compressive buckling characteristics of the stiffened panels can be readily predicted relative to an un-stiffened web plate with increase in the stiffener depth. It is evident from figure 4 that when

the stiffener depth approaches to zero both curves are shown to originate from the same value i.e. $\frac{\sigma_{ycr}}{\sigma_{ycr-unstiffened}} = \frac{\tau_{xycr}}{\tau_{xycr-unstiffened}} = 1$.

The dotted lines at the levels of $\frac{\tau_{xycr}}{\tau_{xycr-unstiffened}} = 1.5133$ and $\frac{\sigma_{ycr}}{\sigma_{ycr-unstiffened}} = 2.5569$ are primarily shown for the comparison purpose.

The shear and compressive buckling strength denoted by dotted lines can be obtained from the simply supported square web plate. However, for the stiffened panel configuration the dotted lines represent the shear and compressive buckling performance of a stiffened panel with a centrally located stiffener that possesses infinite in-plane bending stiffness and zero torsional stiffness. In other words when the stiffener line acts as a nodal line the skin of the stiffened panel with aspect ratio of two is divided into two separate square sub-panels. Therefore the both square sub-panels buckle locally at the point where stiffener is sufficiently deep to hold the stiffener line as a nodal line.

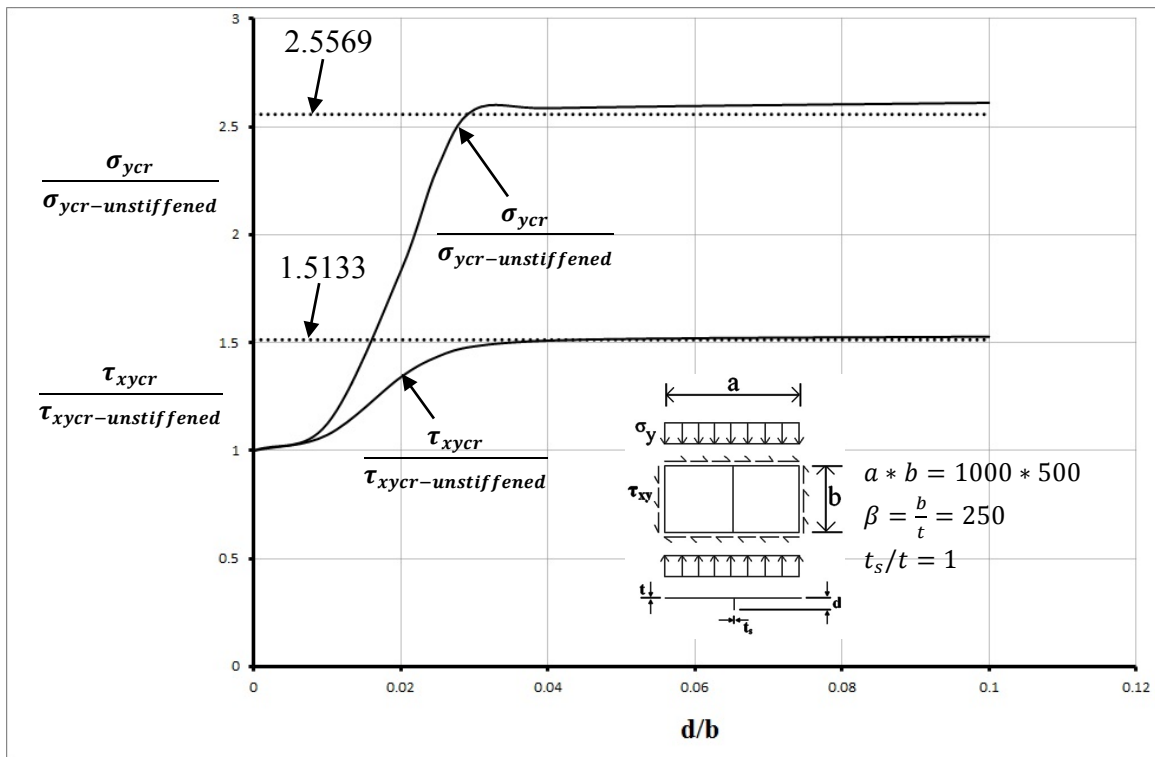


Figure 4: Compression and shear buckling variation with stiffener depth for centrally located single asymmetrical stiffener.

It is clear from the figure 4 that when the stiffeners are considerably deep the both curves are noticed to rise above the dotted lines. This is due to the obvious fact that the stiffener is elastically attached to the skin and there does exit certain degree of rotational restraint at the stiffener-skin juncture depending on the stiffener geometry. Therefore, the dotted lines, which are for zero torsional restraint, are considered to be the lower bound estimates of shear and compressive buckling strengths. Moreover, it can be further observed that with increase in the stiffener depth in the transitional region from general to local buckling the gradient of the curve associated with the compressive loading is noticed to become very steep compared to the that with shear load. The gain in shear strength is, however, found to be gradual in nature. This is basically due to the fact that in general shear buckling mode the stiffener experiences both in-plane bending as well as twisting, whereas in the case of compressive loading the stiffener predominantly undergoes in-plane bending deformation.

The shear and compressive buckling strengths corresponding to $d/b = 0.04$ are found to be of the order of 1.5 and 2.58 times that of un-stiffened web plate respectively. It is to be noticed that the gain in buckling performance for both loading conditions beyond $d/b = 0.04$ is insignificant and therefore it is considered useless to further increase the stiffener depth as it only adds unnecessary weight to the structural system.

The interaction curves for stiffened web panels with single centrally located stiffener subjected to combined compression and shear loading are illustrated in figure 5. The ratio of applied shear stress to the critical shear buckling stress of un-stiffened web plate, $\frac{\tau_{xy}}{\tau_{ycre-unstiffened}}$, is shown to be plotted against the ratio of applied compressive stress to the critical compressive buckling stress, $\frac{\sigma_y}{\sigma_{ycre-unstiffened}}$. Where τ_{xy} and σ_y are simultaneously applied shear and compressive stresses respectively.

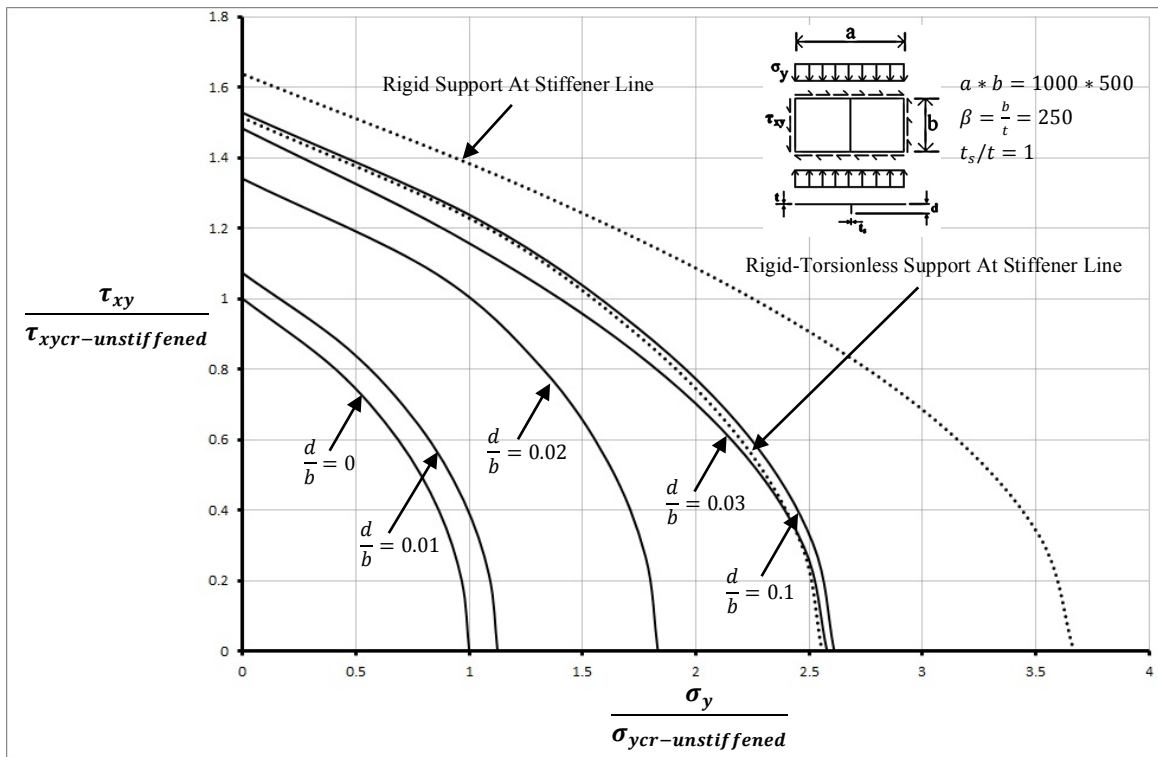


Figure 5: Buckling interaction curves for stiffened panels with a single stiffener under combined compression and shear loading.

It is of note that the curves in figure 4 provide the critical boundary limits (on both horizontal and vertical axis) to the interaction curves shown in figure 5 for the case of combined shear and compression corresponding to the stated stiffener depths. Moreover, the improvement in the buckling capability of the stiffened panel under combined loading with increase in the stiffener depth can be readily determined and compared with that of unstiffened web plate. The curves associated with different stiffener geometries as presented in figure 5, basically, act as critical boundaries of two-dimensional $\sigma_y - \tau_{xy}$ design space.

The stiffener to web depth ratios of 0.01, 0.02, 0.03 and 0.1 are considered. The overall/general buckling mode is noticed to be associated with the stiffener to web depth ratios of 0.01 and 0.02 whereas the general mode is seen to be changed to local buckling mode for the case of $d/b = 0.03$ and 0.1 which ensures that the stiffener is acting as an enforced nodal line. It is clearly manifested from the interaction curves that the design space

is shown to be substantially enlarged with increase in the stiffener depth compared to that of un-stiffened plate. However, the improvement from $d/b = 0.03$ to 0.1 is not found to be significant and therefore further increase in the stiffener depth is considered to be a futile exercise.

The dotted lines shown in figure 5 represent the lower and upper bound estimates of the design space and within these limits only the local buckling of the stiffened panel takes place. The lower bound estimate is associated with the stiffened panel with a stiffener that possesses infinite in-plane bending stiffness but zero torsional stiffness whilst the upper dotted line represents the rigid support at stiffener line which means infinite in-plane bending as well as torsional stiffness (clamped stiffener line). The design curve for $d/b = 0.1$ is noticed to lie above the lower dotted line ensuring that the stiffener is capable of holding the stiffener line (sufficient in-plane bending stiffness). However, it also highlights the poor torsional capability of the stiffener. The torsional stiffness of the stiffener could be improved by increasing the thickness of the stiffener ($t_s/t > 1$) and as a result the curves begin to move towards the upper bound estimate.

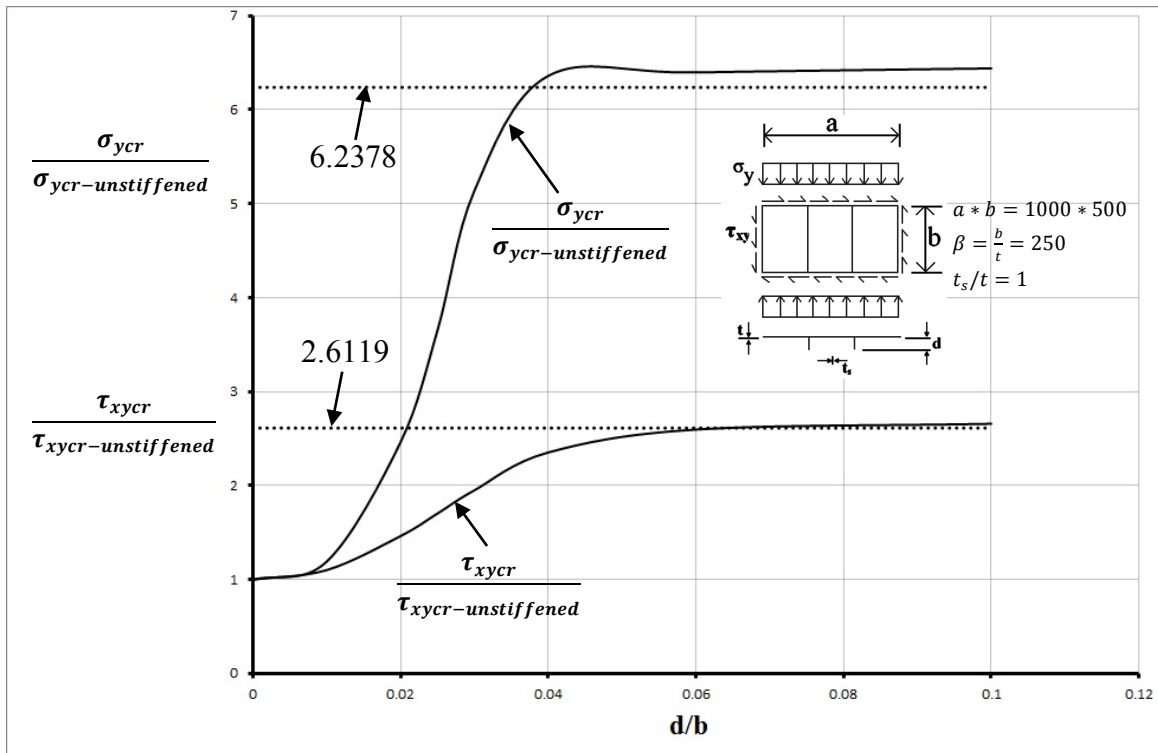


Figure 6: Compression and shear buckling variation with stiffener depth for two equally spaced asymmetrical stiffeners.

Figure 6 illustrates the results for the case of a stiffened panel configuration with two equally spaced stiffeners. The results highlight the effect of change in stiffener depth on independent critical shear as well as on compressive buckling performance. With two equally spaced stiffeners, the skin of the stiffened panel is seen to be divided into three rectangular sub-panels of same size and the ratio of longer to shorter side of each sub-panel is shown to be of the order of 1.5. The dotted lines, drawn mainly for comparative purposes, at the levels of $\frac{\tau_{xycr}}{\tau_{xycr-unstiffened}} = 2.6119$ and $\frac{\sigma_{ycr}}{\sigma_{ycr-unstiffened}} = 6.2378$ demonstrate the shear and compressive buckling performances of a simply supported rectangular web plate with aspect ratio of 1.5 respectively. It can be noted again for the case of two stiffener configuration that the curves begin to rise above the dotted lines at higher stiffener depths ensuring that the

dotted lines represent the lower bound estimate of shear and compressive buckling capabilities with the mode of buckling found to be local in nature.

In the transitional region from general to local buckling mode, the curves associated with shear and compressive stresses shown in figure 6 tend to demonstrate similar behaviour with increase in the stiffener depth to that presented previously in figure 4 for single centrally located stiffener. It is however observed for the case of stiffened panel configuration with two equally spaced stiffeners that the deep stiffeners are required to hold the stiffener lines as the nodal lines in order to enforce the local buckling mode. This is shown to be true particularly for the case of shear loading. Furthermore, it is clearly evident that both the shear and compressive buckling strengths of the stiffened web panels are significantly enhanced due to the presence of an additional stiffener. The critical compressive and shear buckling strengths corresponding to $d/b = 0.06$ are found to be 6.4 and 2.6, respectively, times that of unstiffened web plate whilst the mode of buckling for both types of loadings is local in nature.

The influence of stiffener depth on the critical boundary of the design space associated with different two stiffener configurations is shown in figure 7. The critical compressive and shear buckling stress limits of the interaction curves, shown in figure 7, are obtained from the curves presented in figure 6 corresponding to the specified stiffener depths. The two-dimensional design space is noticed to be significantly enhanced for the case of two equally spaced stiffeners. The interaction curve for $d/b = 0.06$ lies slightly over the lower bound critical boundary which represents the rigid torsionless support at the stiffener line. It is of note that increase in the stiffener depth beyond $d/b = 0.06$, improves the design space marginally and thus $d/b = 0.06$ can be considered as a practical optimum design.

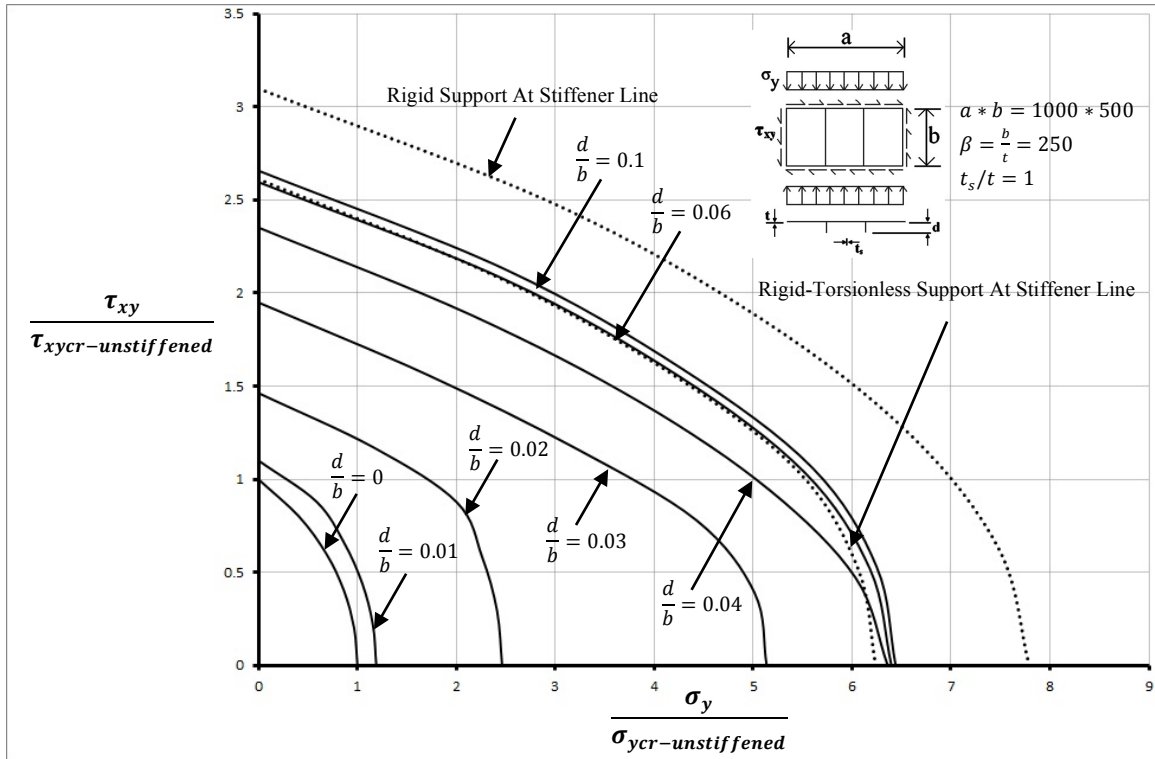


Figure 7: Buckling interaction curves for stiffened panels with two stiffeners under combined compression and shear loading.

4. POST-BUCKLING RESPONSE OF STIFFENED PANELS

4.1. Discussion of results

The finite element modelling strategy is applied to the perforated web plates to determine their post-buckled response and to compare it with the FEA results presented by Paik [14] to validate the proposed simulation approach. The comparison is illustrated in figure 8 and the results shown by the markers are taken from Paik's finite element work whilst the results denoted by dotted lines are obtained from the proposed finite element strategy. The results presented in figure 8 are for simply supported in-plane straight web boundaries of the rectangular perforated steel web plates under combined shear and transverse axial compression. τ_{av}/τ_y is seen to be plotted against the σ_{yav}/σ_y where τ_{av} and σ_{yav} are average shear and transverse compressive stresses respectively. σ_y and τ_y are termed as material yield stress i.e. 352.8 MPa and shear yield stress i.e. $\tau_y = \sigma_y/\sqrt{3}$ respectively. The aspect ratio (a/b) of the webs analysed is 3 with the given dimensions of $2400 * 800$ and the hole diameter to web depth ratio (d/b) is of 0.4. The uniform thickness of the perforated web plate is varied such as 10 mm, 15 mm and 20 mm in order to examine the influence on interaction curves based on ultimate strength. It is evident from figure 8 that the accuracy of finite element simulation strategy is shown to be ascertained considering the fact that the results obtained are found to be in good agreement with those of Paik.

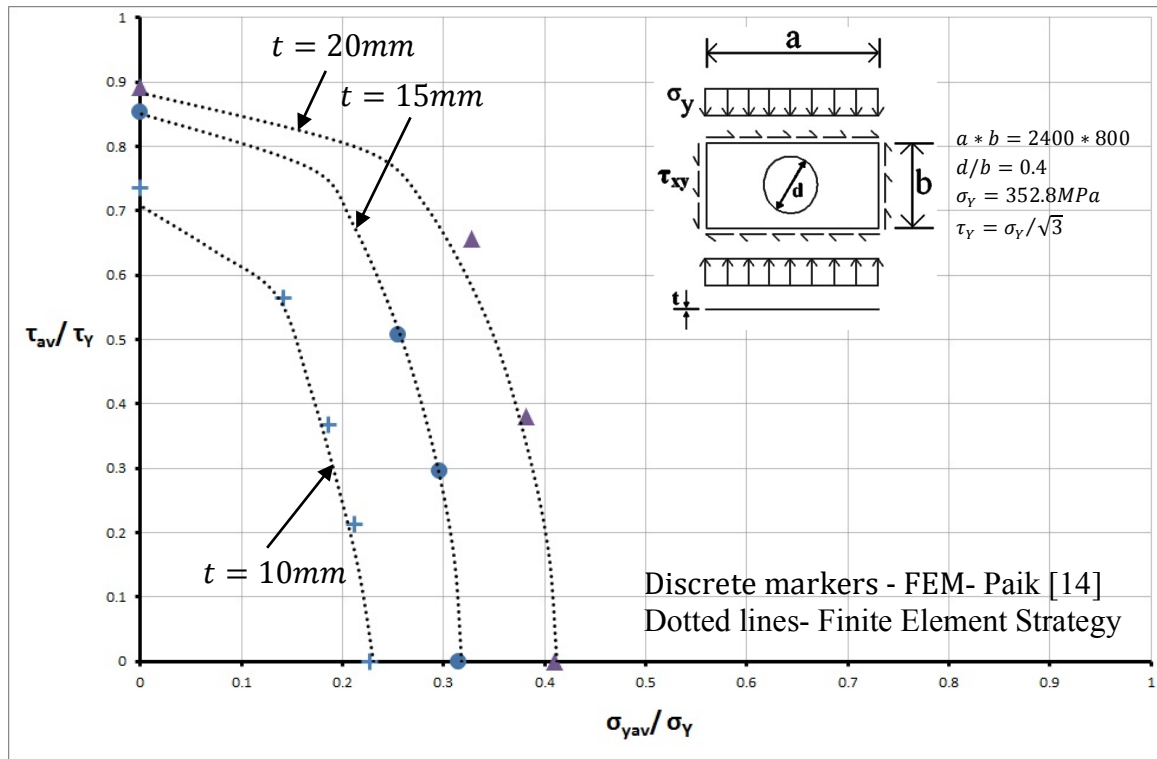


Figure 8: Comparison of FE results with the FE results of Paik [14] for simply supported perforated web plates under combined shear and compression.

The effect of shear preload on the incrementally applied compression, active load, is illustrated in figure 9. Average compressive stress is seen to be plotted against the applied transverse compression in figure 9 whilst considering the effect of applied shear preload. The result shown is for centrally located single asymmetrical stiffener with stiffener to web depth ratio of 0.02. The maximum average compressive stress ($\sigma_{yav} = \sigma_{yu}$), which is of the order of 124.08 N/mm², can be noticed for the case of pure applied compression in the absence of

shear preload. However, when the stiffened panel is subjected to combined loading, the application of constant shear preload results in the reduction of ultimate compressive stress of the stiffened web panel. The ultimate compressive strength continues to degrade with increase in the applied shear preload. The ultimate compressive stresses of the stiffened panel are found to be of the magnitude of 112.78, 94.77, 72.04 and 39.97 N/mm² corresponding to the shear preload values of 0.2 τ_u , 0.4 τ_u , 0.6 τ_u and 0.8 τ_u respectively, where the τ_u is ultimate shear strength of the stiffened panel in the absence of applied compression. Similar results are obtained for other stiffener configurations but are not reported here. It is evident from figure 9 that the finite element modelling strategy and solution procedures, which are proposed for the structural systems subjected to combined shear and compression, are effectively capable of taking into account all the aspect of complete loading history including the compression drop off stage.

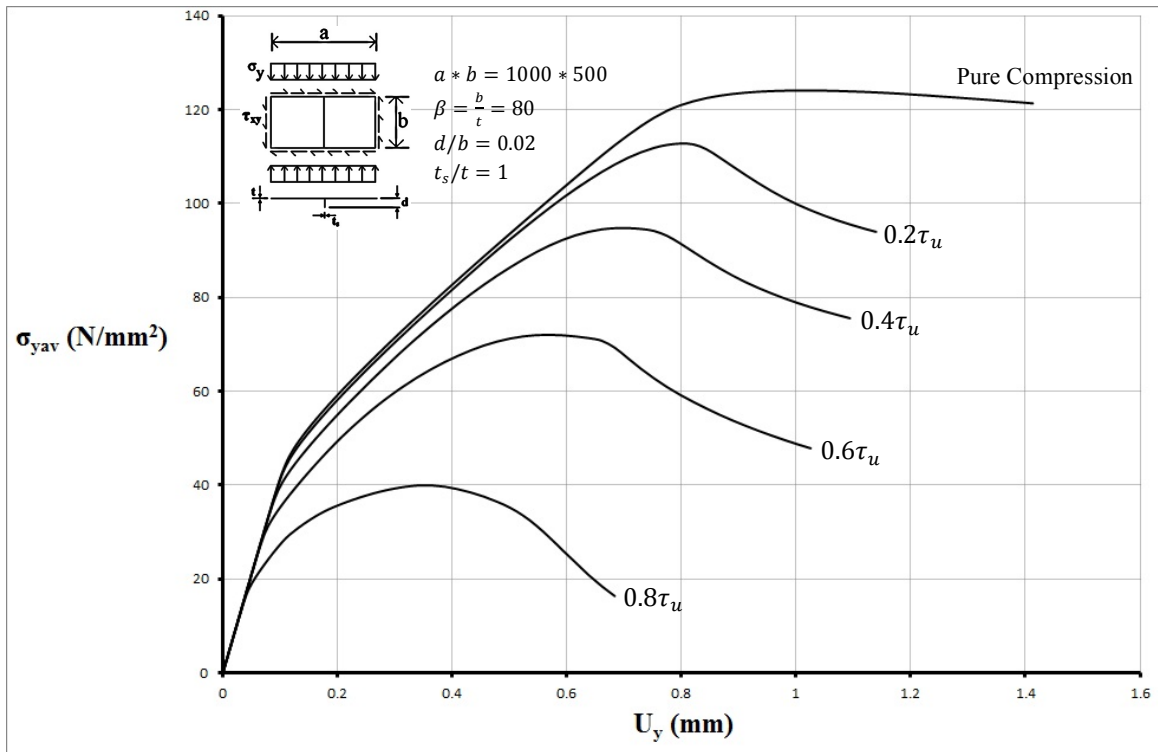


Figure 9: Average compressive stress, σ_{yav} , against the applied transverse compression, U_y , for stiffener to web depth ratio of 0.02.

The ultimate strength interaction curves for stiffened web panels subjected to combined compression and shear loading are shown in figure 10. The ratio of applied shear stress to the ultimate shear stress of an un-stiffened web plate, $\frac{\tau_{xy}}{\tau_{u-unstiffened}}$, is seen to be plotted against the ratio of applied compressive stress to the ultimate compressive stress, $\frac{\sigma_y}{\sigma_{yu-unstiffened}}$. Where τ_{xy} and σ_y are simultaneously applied in-plane shear and compressive stresses respectively. The gain in ultimate strength of the stiffened panels under combined loading can be readily noticed relative to un-stiffened web plate corresponding to different stiffener geometries. The interaction curves associated with different stiffener to web depth ratios as shown in figure 10 are essentially considered as ultimate boundaries of two-dimensional $\sigma_y - \tau_{xy}$ design space. The stiffener to web depth ratios (d/b) of 0.02, 0.04, 0.06, 0.08 and 0.1 are considered. The mode shapes, which are noticed in the post-buckling range for various stiffener geometries under the combined loading, are not mostly found to be identical to those

under pure shear and compression. The behaviour of post-buckling mode shapes for any specific stiffener geometry varies depending on the extent of applied shear preload.

It is clearly evident from figure 10 that the two-dimensional design space of interaction curves is considerably enhanced with increase in the stiffener depth. However, it is to be observed that the improvement in the design space is primarily due to the gain in compressive strength with increase in the stiffener depth. Whilst the ultimate shear strength is shown to be slightly improved corresponding to $d/b = 0.02$ and further increase in the stiffener depth does not notably change the shear strength. Moreover, the improvement in compressive strength is not found to be of substantial order with increase in the stiffener to web depth ratio beyond 0.1 and thus further increase in the stiffener depth is not recommended based on the practical design considerations.

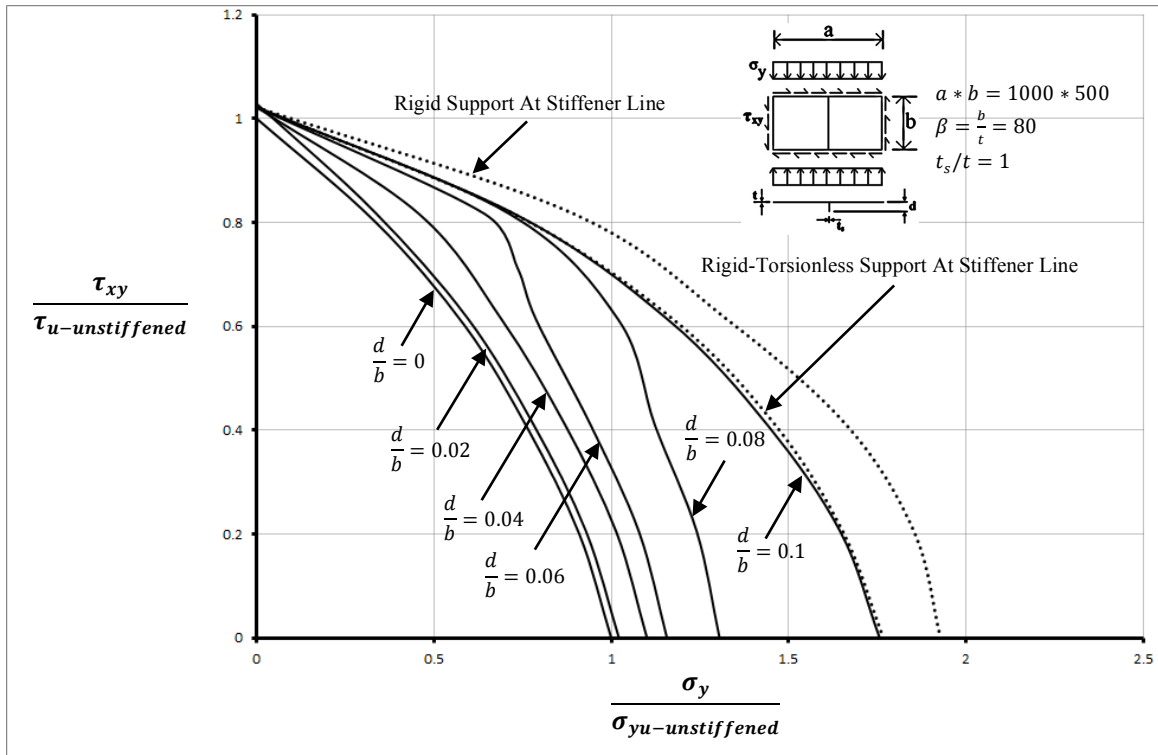


Figure 10: Ultimate strength interaction curves for the stiffened panels with a single stiffener under combined compression and shear loading.

The dotted lines in figure 10 represent the lower and upper bound estimates of ultimate strength interaction curves. The lower bound result is obtained when the stiffener is assumed to have infinite in-plane bending stiffness and zero torsional stiffness. Similarly the upper bound outcome corresponds to the situation in which the stiffener possesses infinite in-plane bending stiffness and infinite torsional stiffness. Therefore, the buckling mode shape of the stiffened panels in the region present within the dotted lines is always noted to be local in nature. The interaction curve with regard to $d/b = 0.1$ is shown to almost coincide with the lower dotted line, which ensures that the stiffener with $d/b = 0.1$ is able to effectively hold the stiffener line throughout the loading process despite the lack of torsional capability. The torsional capability can be improved by increasing the stiffener thickness and consequently the curves begin to move towards the upper dotted line. It is significant to notice that the effect of improvement in torsional stiffness results in increase of the ultimate compressive stress only and the shear strength remains unchanged.

The ultimate strength interaction curves for stiffened web panels with two equally spaced stiffeners subjected to combined shear and compressive loading are illustrated in figure 11. The stiffener to web depth ratios (d/b) of 0.02, 0.04, 0.07, 0.08 and 0.1 are considered. It is obvious from figure 11 that the two-dimensional interactive design space is significantly increased with increase in the stiffener depth. The similarity noticed between the interaction curves of the stiffened panels with centrally located single and equally spaced two stiffeners is that the enhancement of the design space is basically due to the improvement in the ultimate compressive strength with increase in the stiffener depth. The ultimate compressive stress corresponding to $d/b = 0.1$ cannot be improved further by only increasing the stiffener depth considering the fact the stiffeners already possess in-plane bending stiffness required to hold the stiffener line as nodal line. Thus the interactive curve with regard to $d/b = 0.1$ only begins to move towards the upper bound interactive dotted curve if the torsional capability of the stiffeners is improved by increasing the stiffener thickness ($t_s/t > 1$).

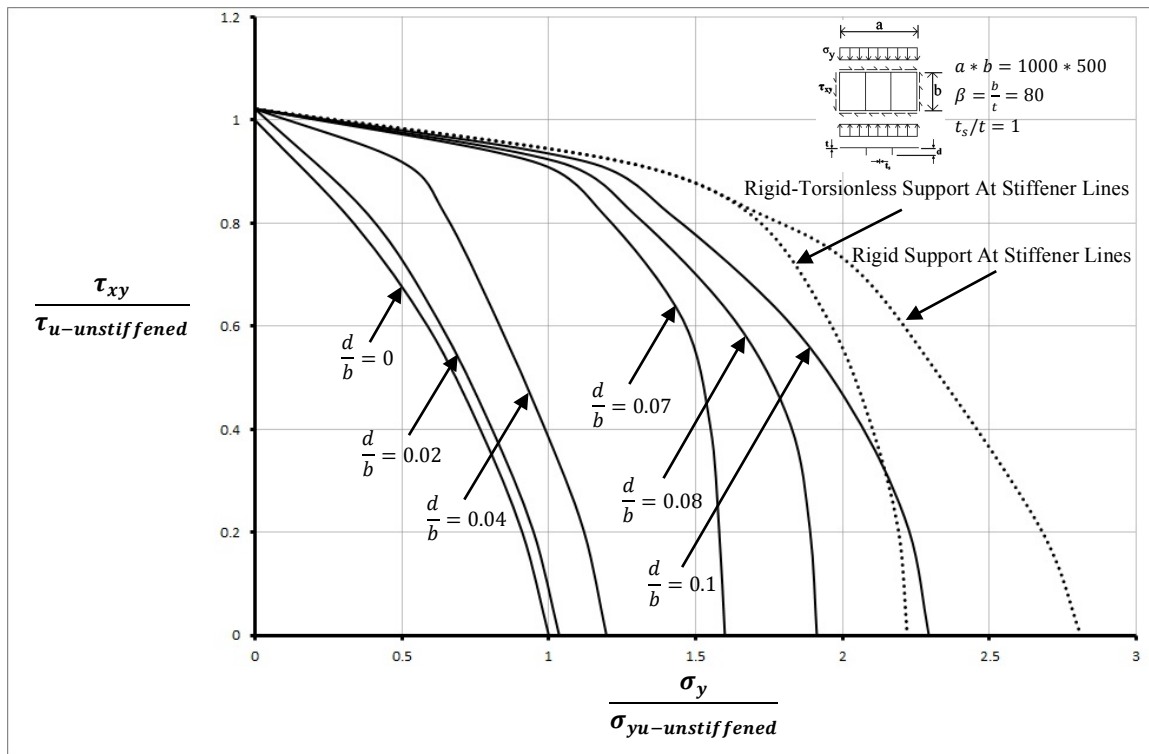


Figure 11: Ultimate strength interaction curves for the stiffened panels with two equally spaced stiffeners under combined compression and shear loading.

5. CONCLUSION

This paper details the finite element simulation strategies and solution procedures that are effectively applied to different structural configurations subjected to combined shear and compression. The facility SOL105 in MSC NASTRAN enables the application of combined loading through the execution of the STATSUB command in which one of the loadings is considered as a constant preload while the other acts as an active load. This finite element modelling approach, validated against the analytical work of Bulson [2], is shown to be able to accurately predict the buckling performance of the stiffened web panels under combined loading. Critical buckling interaction curves are presented for different stiffener geometries for the case of centrally located single and equally spaced two stiffeners configurations.

However, for the incremental nonlinear analysis, unlike SOL 105, the SOL 106 facility of MSC NASTRAN does not automatically permit one to have a constant preload right from the beginning of the applied incremental loading. Therefore, a new strategy has been developed for the application of combined shear and compression loading in which the shear load in the form of a uniformly distributed force acts as a constant preload and its value remains unchanged throughout the solution run, whilst, compression in the form of an enforced displacement is applied incrementally through the complete loading process. This approach has shown to be employed to investigate the structural response of the stiffened panels in the post-buckling range. Two dimensional interaction curves based on ultimate performance of the stiffened panels under combined loading are presented for different stiffener configurations. This finite element modelling approach, validated against the work of Paik [14], is found to be efficient to accurately predict the compressive response of the stiffened panels in the presence of constant shear preload and is able to capture all the aspects throughout the loading history from the onset of initial buckling through the elastic and elasto-plastic post-buckling phase of behaviour to the ultimate conditions followed by the subsequent elasto-plastic unloading phase.

REFERENCES

- [1]. Plank, R. J., Williams, F. W. "Critical buckling of some stiffened panels in compression, shear and bending." Aeronautical Quarterly, 1974, pp. 165–179.
- [2]. Bulson, P. S., "*The stability of flat plates*", London: Chatto & Windus, 1970.
- [3]. Loughlan, J. "The Buckling and Vibrational Behaviour of some Stiffened Panels Subjected to In Plane Shear Loading." Proceedings of Applied Solid Mechanics - 4, Ponter, A.R.S. and Cocks, A.C.F. (eds), Elsevier Applied Science Publishers, University of Leicester, UK, 1991, pp 275-302.
- [4]. Loughlan, J. "The buckling performance of composite stiffened panel structures subjected to combined in-plane compression and shear loading." Composite Structures, 1994, Volume 29, Issue 2, Pages 197-212.
- [5]. Ueda, Y., Rashed, S. M. H., and Paik, J. K. "Buckling and ultimate strength interaction in plates and stiffened panels under combined in-plane biaxial and shearing forces." Marine Structures, 1995, Volume 8, Issue 1, Pages 1-36.
- [6]. Lee S. C., Yoo C. H., and Yoon D. Y. "Behaviour of intermediate transverse stiffeners attached on web panels." Journal of Structural Engineering ASCE; 2002, 128(3):337–45.
- [7]. Lee S. C., Yoo C. H., and Yoon D. Y. "New design rule for intermediate transverse stiffeners attached on web panels." J Struct. Eng.; 2003, 129(12):1607–1614.
- [8]. Xie, M., Chapman, J. C. "Design of web stiffeners: axial forces." Journal of Constructional Steel Research, 2003, Volume 59, Issue 8, Pages 1035-1056.
- [9]. Byklum, E., Steen, E., and Amdahl, J. "A semi-analytical model for global buckling and postbuckling analysis of stiffened panels." Thin-Walled Structures, 2004, Volume 42, Issue 5, Pages 701-717.
- [10]. Alinia, M. M. "A study into optimization of stiffeners in plates subjected to shear loading." Thin-Walled Structures, 2005, Volume 43, Issue 5, Pages 845-860.
- [11]. Murphy, A., Price, M., Lynch, C., and Gibson, A. "The computational post-buckling analysis of fuselage stiffened panels loaded in shear." Thin-Walled Structures, 2005, Volume 43, Issue 9, Pages 1455-1474.
- [12]. Featherston, C. A., Koffi, K., and Burguete, R. L. "Postbuckling behaviour of a stiffened panel subject to combined loading." In: Proceedings of the 25th ICAS Congress, Hamburg, Germany, 2006.
- [13]. Paik, J. K., "Ultimate strength of perforated steel plates under edge shear loading", Thin-Walled Structures, 2007, Vol. 45(3), pp. 301-306.

- [14].Paik, J. K., "Ultimate strength of perforated steel plates under combined biaxial compression and edge shear loads", *Thin-Walled Structures*, 2008, Vol. 46(2), pp. 207-213.
- [15].Alinia M. M., Shirazi R. S. "On the design of stiffeners in steel plate shear walls." *J Constr. Steel Res*; 2009, 65:2069-2077.
- [16].Loughlan, J., Hussain, N. "The in-plane shear failure of transversely stiffened thin plates", *Thin-Walled Structures*, 2014, Volume 81, pp. 225-235.